Optical negative-index metamaterials

Artificially engineered metamaterials are now demonstrating unprecedented electromagnetic properties that cannot be obtained with naturally occurring materials. In particular, they provide a route to creating materials that possess a negative refractive index and offer exciting new prospects for manipulating light. This review describes the recent progress made in creating nanostructured metamaterials with a negative index at optical wavelengths, and discusses some of the devices that could result from these new materials.

VLADIMIR M. SHALAEV

School of Electrical and Computer Engineering and Birck Nanotechnology Center, Purdue University, West Lafayette, Indiana 47907, USA.

e-mail: shalaev@purdue.edu

Light is the ultimate means of sending information to and from the interior structure of materials — it packages data in a signal of zero mass and unmatched speed. However, light is, in a sense, 'one-handed' when interacting with atoms of conventional materials. This is because from the two field components of light — electric and magnetic — only the electric 'hand' efficiently probes the atoms of a material, whereas the magnetic component remains relatively unused because the interaction of atoms with the magnetic-field component of light is normally weak. Metamaterials, that is, artificial materials with rationally designed properties, can allow both field components of light to be coupled to meta-atoms, enabling entirely new optical properties and exciting applications with such 'two-handed' light. Among the fascinating properties is a negative refractive index. The refractive index is one of the most fundamental characteristics of light propagation in materials. Metamaterials with negative refraction may lead to the development of a superlens capable of imaging objects and fine structures that are much smaller than the wavelength of light. Other exciting applications of metamaterials include antennae with superior properties, optical nanolithography and nanocircuits, and 'metacoatings' that can make objects invisible.

The word 'meta' means 'beyond' in Greek, and in this sense the name 'metamaterials' refers to 'beyond conventional materials'. Metamaterials are typically man-made and have properties that are not found in nature. What is so magical about this simple merging of 'meta' and 'materials' that has attracted so much attention from researchers and has resulted in exponential growth in the number of publications in this area?

The notion of metamaterials, which includes a wide range of engineered materials with pre-designed properties, has been used, for example, in the microwave community for some time. The idea of metamaterials has been quickly adopted in optics research, thanks to rapidly developing nanofabrication and subwavelength imaging techniques. Metamaterials are expected to open a new gateway to unprecedented electromagnetic properties and functionality unattainable from naturally occurring materials. The structural units of metamaterials can be tailored in shape and size. Their composition and morphology can be artificially tuned, and inclusions can be designed and placed at desired locations to achieve new functionality. One of the most exciting opportunities for metamaterials is the development of negative-index materials (NIMs). These NIMs bring the concept of refractive index into a new domain of exploration and thus promise to create entirely new prospects for manipulating light, with revolutionary impacts on present-day optical technologies.

The arrival of NIMs provides a rather unique opportunity for researchers to reconsider and possibly even revise the interpretation of very basic laws. The notion of a negative refractive index is one such case. This is because the index of refraction enters into the basic formulae for optics. As a result, bringing the refractive index into a new domain of negative values has truly excited the imagination of researchers worldwide.

The refractive index is a complex number $n = n' + in''$, where the imaginary part n'' characterizes light extinction (losses). The real part of the refractive index n' gives the factor by which the phase velocity of light is decreased in a material as compared with vacuum. NIMs have a negative refractive index, so the phase velocity is directed against the flow of energy in a NIM. This is highly unusual from the standpoint of 'conventional' optics. Also, at an interface between a positive- and a negative-index material, the refracted light is bent in the 'wrong' way with respect to the normal. Furthermore, the vectors **E**, **H** and **k** form a left-handed system (hence NIMs are also called 'left-handed' materials).

Despite all these unusual properties, it is probably not that surprising to learn that a few scientific giants considered phenomena related to NIMs quite some time ago. Their studies were perhaps so early that they could not be fully appreciated by their contemporaries. Negative phase velocity and its consequences were discussed in works by Sir Arthur Schuster[1] and H. Lamb[2] as early as 1904. Later the optical properties of NIMs were studied by Russian physicists L. I. Mandel'stam[3], D. V. Sivukhin[4], and V. G. Veselago[5]. Veselago has provided the modern prescription of 'negative permittivity/negative permeability' for negative refraction, and he carried through the ramifications of this to many optical phenomena. The recent boom in NIMs was inspired by Sir John Pendry, who made a number of critical contributions to the field including his famous prediction of the NIM-based superlens with resolution beyond the diffraction limit[6] (see Box 1).

No naturally existing NIM has yet been discovered for the optical range of frequencies, where the properties of 'two-handed' light could be particularly spectacular. Therefore, it is necessary to turn to man-made, artificial materials that are composed in such a way that the effective refractive index is less than zero, $n'_{eff} < 0$.

REVIEW ARTICLE

Box 1 Superlenses

Among the most exciting applications of NIMs is the 'perfect' lens proposed by Pendry[6], who pointed out that a slab with refractive index $n = -1$ surrounded by air allows the imaging of objects with subwavelength precision (see Fig. B1). Provided that all of the dimensions of a system are much smaller than the wavelength, the electric and magnetic fields can be regarded as quasi-static and independent, and the requirement for superlensing is reduced to only $\varepsilon = -\varepsilon_h$, where ε_h is the permittivity of the host medium interfacing the lens ($\varepsilon_h = 1$ for air). Although limited to the near-field zone only, this kind of near-field superlens (NFSL) still enables many interesting applications including those of biomedical imaging and subwavelength photolithography. A slab of silver illuminated at its surface-plasmon resonance frequency (where $\varepsilon = -\varepsilon_h$) is a good candidate for such an NFSL. Experiments with silver slabs have already shown growth of evanescent waves[95] and imaging beyond the diffraction limit[79–81]. A near-field superlens operating in the mid-infrared part of the spectrum has also been demonstrated[82].

We note, however, that an NFSL can operate only at a single frequency ω satisfying the lens condition $\varepsilon(\omega) = -\varepsilon_h$, which is indeed a significant drawback for a lens based on bulk metals. It has been shown that by using metal–dielectric composites instead of bulk metals, one can develop an NFSL operating at any desired visible or near-infrared wavelength, with the frequency controlled by the metal filling factor of the composite[83]. Finally, we mention here the recent, promising ideas to convert the evanescent-field components into propagating modes, allowing super-resolution in the far zone without optical magnetism[84–86].
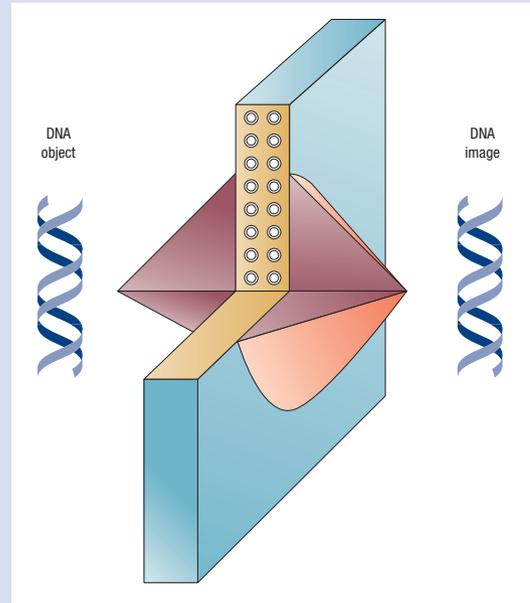

Figure B1 A superlens could perform high-resolution imaging of an object. Red cones indicate the trajectory of the light. (Courtesy of X. Zhang)

There are several approaches to obtaining NIMs, such as photonic crystals (see, for example, refs 7–14), transmission lines[15] and their optical analogues[16]. Owing to space limitations, however, this review is purely focused on the recent efforts to develop optical NIMs by using metal–dielectric nanostructures.

The optical properties of materials are governed by two material constants: the permittivity ε and the permeability μ, describing the coupling of a material to the electric- and magnetic-field components of light, respectively. A possible (but not the only) approach to achieving a negative refractive index in a passive medium is to design a material where the (isotropic) permittivity, $\varepsilon = \varepsilon' + i\varepsilon''$, and the (isotropic) permeability, $\mu = \mu' + i\mu''$, obey the equation $\varepsilon'|\mu| + \mu'|\varepsilon| < 0$ (refs 17 and 18). This leads to a negative real part of the refractive index $n = n' + in'' = \sqrt{\varepsilon\mu}$.

The inequality above is always satisfied if both $\varepsilon' < 0$ and $\mu' < 0$. However, we note that this is not a necessary condition. There may be magnetically active media (that is, $\mu \neq 1$) with a positive real part μ' for which the inequality is fulfilled and which therefore show a negative real part of the refractive index n'. However, the figure of merit $F = |n'| / n''$ in the latter case is typically small.

We also mention here that besides the '$\varepsilon(\omega)$ and $\mu(\omega)$' approach for NIMs used here, there is also an alternative description[19] based on the generalized, spatially dispersive permittivity $\varepsilon_{\alpha\beta}(\omega, k)$; in this case, the non-local tensor $\varepsilon_{\alpha\beta}(\omega, k)$ describes both electrical and magnetic responses.

Above, we considered isotropic media where ε and μ are complex scalar numbers. It has been shown that in the case of anisotropic media, where ε and μ are tensors, a negative refractive index is feasible even if the material, which is placed in a waveguide, shows no magnetic response ($\mu = 1$). For example, $n' < 0$ can be achieved for a uniaxial dielectric constant with $\varepsilon_x = \varepsilon_\perp < 0$ and $\varepsilon_y = \varepsilon_z = \varepsilon_\parallel > 0$

(ref. 20). Other suggestions for negative refraction in waveguides have been proposed[16,21]. Despite the fact that using anisotropic media and special waveguide structures are promising approaches, we will not consider these topics here. This is mainly because a negative index for optical frequencies has only been achieved thus far by following the approach of magnetically active media.

Below we focus on the recent progress in scaling magnetism and negative refraction up to the optical frequencies, and discuss some of the unusual properties of optical metamaterials.

OPTICAL MAGNETISM

For materials at optical frequencies, the dielectric permittivity ε is different from that in vacuum. In contrast, the magnetic permeability μ for naturally occurring materials is close to its free-space value in the optical range. This is because the magnetic-field component of light couples to atoms much more weakly than the electric component, making light 'one-handed' as discussed above. The magnetic coupling to an atom is proportional to the Bohr magneton $\mu_B = e\hbar/2m_ec = \alpha ea_0/2$ (where e is the electron charge, $\hbar$ is the reduced Planck constant, m_e is the electron mass, a_0 is the Bohr radius) and the electric coupling is ea_0. The induced magnetic dipole also contains the fine-structure constant $\alpha \approx 1/137$ so that the effect of light on the magnetic permeability is α^2 weaker than on the electric permittivity. This also explains why all naturally occurring magnetic resonances are limited to relatively low frequencies. As a magnetic response is a precursor for negative refraction, it is of critical importance to address the fundamental problem above by engineering optical magnetism.

The problem of low coupling to the magnetic-field component of light can be overcome by using metamaterials that mimic magnetism
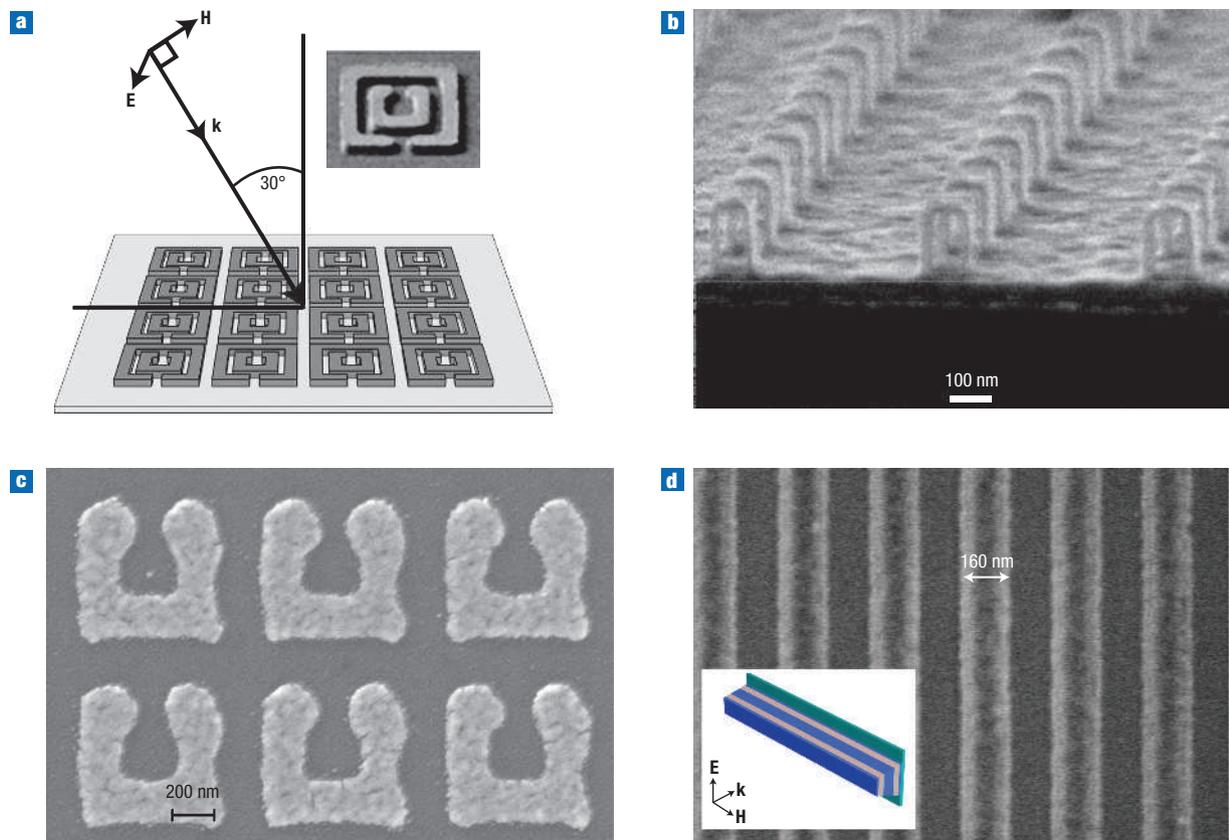
Figure 1 Terahertz and optical-magnetic structures. **a**, Double SRR structure with terahertz magnetic response. Reprinted with permission from ref. 25. Copyright (2004) AAAS. **b**, Staple-shaped nanostructure with a mid-infrared magnetic resonance. Reprinted with permission from ref. 26. Copyright (2005) APS. **c**, The single planar SRR structure where a negative permeability is obtained at 85 THz. Reprinted with permission from ref. 27. Copyright (2004) AAAS. **d**, Array of paired silver strips providing negative permeability in the visible at $\lambda \approx 725$ nm (ref. 31).

at high frequencies. For the gigahertz range, a solution was suggested by Pendry[22] in which two concentric split-ring resonators (SRRs) of subwavelength dimensions, facing in opposite directions were predicted to give rise to $\mu' < 0$. This can be regarded as an electronic circuit consisting of inductive and capacitive elements. The rings form the inductances and the two slits as well as the gap between the two rings can be considered as capacitors. A magnetic field oriented perpendicular to the plane of the rings induces an opposing magnetic field in the loop owing to Lenz's law. This leads to a diamagnetic response and hence to a negative real part of the permeability.

SRRs operating in the gigahertz regime were first demonstrated by Smith, Schultz *et al.*[23,24] and had a diameter of several millimetres. Scaling this design down in size leads to a response at higher frequencies. The resonance frequency has been pushed up to 1 THz using this scaling technique[25] (see Fig. 1a). An alternative to double SRRs is to fabricate a staple-like structure facing a metallic mirror[26] (Fig. 1b), which enables the resonance frequency to be shifted to 60 THz. As demonstrated by Linden and co-workers[27], single SRRs that show an electric response at 85 THz can also provide a magnetic response at this frequency range (see Fig. 1c). The magnetic response of U-shaped structures has been pushed[28] to the important telecom wavelength of 1.5 µm.

Following theoretical prediction in ref. 29 (a similar structure was also proposed in ref. 30), a negative magnetic response with $\mu' = -1.7$ at a wavelength $\lambda = 725$ nm, has been obtained in arrays of pairs of parallel silver strips[31] (Fig. 1d), which is within the visible range. (As defined by the International Commission on Illumination, the

visible range extends from 380 nm to 780 nm; ref. 32) The magnetic response in the pairs of metal strips results from asymmetric currents in the metal structures induced by the perpendicular magnetic-field component of light[29]. The pairs of metal strips are closely related to pairs of rods, for which the optical diamagnetic response (along with a negative refractive index) was first predicted[33] in 2002 (see below). By simply sliding the pairs of rods in the x–y plane parallel to each other, pairs of strips are obtained. For both structures, pairs of rods and pairs of strips, the optical magnetic response results from the asymmetric currents induced by the magnetic-field component.

We note that the claims of negative μ' in ref. 34 and negative n' in ref. 35 for pairs of gold pillars at the green-light wavelength were not verified after detailed simulations performed by two research groups, who showed that in the system described in refs 34 and 35 both μ' and n' were positive in the visible part of the spectrum[36]. Thus, the shortest wavelength at which $\mu' < 0$ has been observed so far is red, at $\lambda = 725$ nm; ref. 31.

The experiments above were critical for the field because they demonstrated optical magnetism; still, no negative refractive index was observed in those experiments.

NEGATIVE REFRACTIVE INDEX IN OPTICS

The electromagnetic response of metals in the optical range is vastly different from those at lower frequencies, where ε is extremely large and metals behave as nearly perfect conductors. At
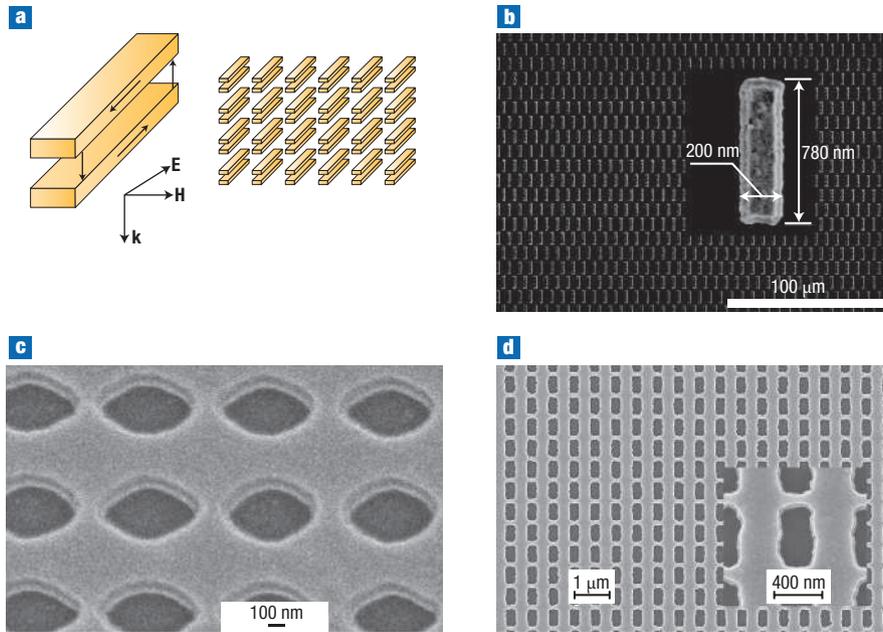
Figure 2 Optical negative-index materials. **a**, Schematic of an array of paired nanorods supporting antiparallel current modes. **b**, Field-emission scanning electron microscope images of the fabricated array where a negative refractive index is achieved at telecommunication wavelengths. **c**, Arrays of ellipsoidal voids in a pair of metal sheets with a negative index at about $\lambda = 2 \, \mu$m. **d**, The nano-fishnet where the largest figure of merit $F = 3$ was obtained at $\lambda \approx 1.4 \, \mu$m. Figures reprinted with permission from ref. 37 (**a,b**), ref. 43 (**c**), ref. 44 (**d**). All copyright OSA.

optical frequencies, ε in metals can be comparable to the dielectric permittivity of a host material, allowing the excitation of a surface-plasmon resonance that opens new means of achieving negative permittivity and permeability.

Although first obtained in the microwave range[23,24], scaling negative refraction up to the optical range is indeed important because it enables exciting applications of NIMs. The first experimental demonstrations of negative refractive index in the optical range were accomplished, nearly at the same time, for pairs of metal rods[37] (Fig. 2a and b) and for the inverted system of pairs of dielectric voids in metal[38] (Fig. 2c).

It was shown in an early paper by Lagarkov and Sarychev[39] that a pair of metal nanorods can have a large paramagnetic response. Then, Podolskiy et al.[33] showed that such a pair of metal nanorods is also capable of a diamagnetic response and, most importantly, negative n' in the optical range. Later, this approach has been discussed in more detail[40,41] . As is illustrated in Fig. 2a, a pair of nanorods can show a negative response to an electromagnetic plane wave. An a.c. electric field parallel to both rods induces parallel currents in both rods. The magnetic field, which is oriented perpendicular to the plane of the rods, causes antiparallel currents in the two rods as shown in Fig. 2a. These antiparallel currents cause the magnetic response of the system (a similar mechanism works for the strips considered in Fig. 1d). The magnetic response will be dia- or paramagnetic depending on whether the wavelength of the incoming magnetic field is shorter or longer than the magnetic resonance of the coupled rods. The metal rods can also be thought of as inductors, where the gaps at the ends form two capacitors. The overall result is a resonant LC circuit with a current loop that operates at optical frequencies[33,39,42].

A negative refractive index of $n' = -0.3 \pm 0.1$ in the optical range was observed in 2005 at the telecommunication wavelength $\lambda = 1.5 \, \mu$m in an electron-beam-fabricated sample of paired rods (Fig. 2b)[37]. We note that F was low in this first experiment. A relatively high F (exceeding one) can normally be obtained only when both ε' and μ' are negative at the same frequency, which is typically hard to accomplish for a simple structure such as pairs of rods (see the discussion below on various means to overcome this problem). A negative refractive index $n' < 0$ in the first experiments[37,38] was accomplished in part because of the significant contribution from the imaginary part of the magnetic permeability μ'', which typically does not allow large F.

A promising approach to NIM design is to use the inverse of a resonant structure[37], for example, a pair of voids as the inverse of a pair of nanorods[38,43] (Fig. 2c). Let us look at an array of pairs of metal nano-ellipses separated by a dielectric, which are similar to the pairs of rods in Fig. 2a. The inverse of this design would be paired elliptically shaped voids in metal films. To make such a structure, we can begin with two thin films of metal separated by a dielectric. Then, elliptically shaped voids etched in the two metal films form the inverse of the original structure of paired metal ellipses. Both such samples, in accordance with the Babinet principle, should have similar resonance behaviour if the orientation of the electric and magnetic fields are also interchanged. Using this approach, Zhang et al. have obtained a negative refractive index in the range of $\lambda \approx 2 \, \mu$m, first for circular voids (with a relatively small figure of merit $F = 0.5$; ref. 38), and later for elliptical voids (with a rather large figure of merit of $F = 2$; ref. 43).

So far, the largest figure of merit for negative refractive index materials in the optical range was achieved by the Karlsruhe group in collaboration with Iowa State University[44] (see Fig. 2d). It was obtained for a fishnet structure, which was considered theoretically in ref. 45 and can be viewed as simply pairs of rectangular dielectric voids in parallel metal films (rather than circular voids as in ref. 38, or elliptical voids as in ref. 43). In the fishnet structure, the pairs of broader metal strips provide negative permeability by means of the asymmetric currents (as considered above, Fig. 1d and refs. 29, 31 and 33), whereas the pairs of narrower metal strips (wires) give

Table 1 Negative refractive index in optics

Year and reference	Refractive index, n'	Wavelength, λ (μm)	Figure of merit, $F = |n'|/n''$	Structure used
2005				
37	−0.3	1.5	0.1	Paired nanorods
38	−2	2.0	0.5	Nano-fishnet with circular voids
2006				
43	−4	1.8	2.0	Nano-fishnet with elliptical voids
44	−1	1.4	3.0	Nano-fishnet with rectangular voids
47	−0.6	0.78	0.5	Nano-fishnet with rectangular voids

a negative permittivity. The Karlsruhe–Iowa State group observed a large negative refractive index, reaching $n' = -2$ at $\lambda \approx 1.45$ μm, and an impressive figure of merit reaching $F = 3$ at $\lambda = 1.4$ μm. By using pulsed interferometry, they were also able to measure both the phase and group velocities of light in their structure[46]. Finally, the same group recently reported $n' = -0.6$ at 780 nm, with a relatively low $F = 0.5$ because μ' was still positive in this spectral range[47].

Table 1 summarizes observations of negative refractive index in optics to date. All successful designs for negative refractive index in the optical range have so far used the idea of creating a negative magnetic permeability by means of the excitation of asymmetric currents in pairs of either rods or strips, following the original idea in ref. 33. The negative permittivity in such structures originates from resonant or off-resonant oscillations of electrons in metals.

As mentioned above, it is typically difficult to obtain both electric and magnetic resonances in the same frequency range. A possible solution to this generic problem is to use a resonant magnetic structure along with a non-resonant metal structure that provides 'background' negative permittivity in a broad spectral range, including the wavelength where the magnetic resonance occurs. This is easy to achieve as noble metals such as gold and silver have negative permittivity at optical frequencies below the plasma frequency. Hence, merely adding, for example, a metal film above and below the magnetic resonator should provide negative permittivity (see Fig. 3a). An alternative method to achieve the background negative permittivity is to use pairs of continuous metal wires[48], which do not have an electrical resonance at the wavelength of interest. Then a magnetic resonance is obtained by including appropriately designed pairs of rods (or 'cut wires', as the authors of ref. 48 call them), see Fig. 3b. We note that in the fishnet structure discussed above, the pairs of the narrower strips act as such off-resonant wires and, at the wavelength where the magnetic resonance occurs in the broader strips, they simply provide a background negative permittivity.

Simulations show that combining continuous metal films with nanostrip magnetic resonators could easily yield a negative-index material[49]. Unfortunately, this requires metal films that are too thin to be fabricated with current technology. The problem arises because noble metals have a highly negative real part of their permittivity (for example, around 1.5 μm), and the magnetic resonator cannot provide a comparable value of negative permeability. This results in a huge impedance mismatch and subsequently a large reflection that degrades the magnetism of the entire structure.

To address this issue, the film can be formed with a mixture of dielectric (for example, silica) and metal, such as silver or gold, forming a semicontinuous metal film (SMF)[49]. Such SMFs can be fabricated using very basic techniques such as the evaporation of metal onto a dielectric substrate. For example, consider the structure in Fig. 3a, where semicontinuous silver–silica films are
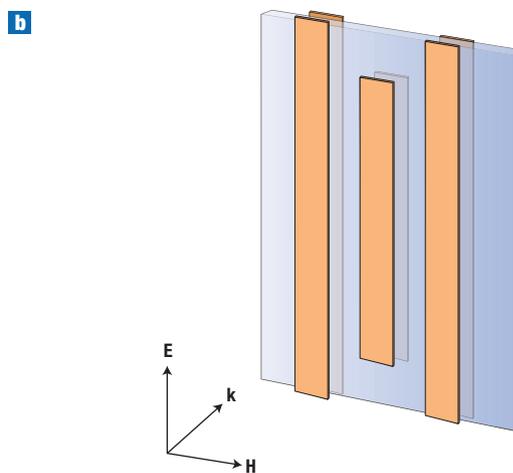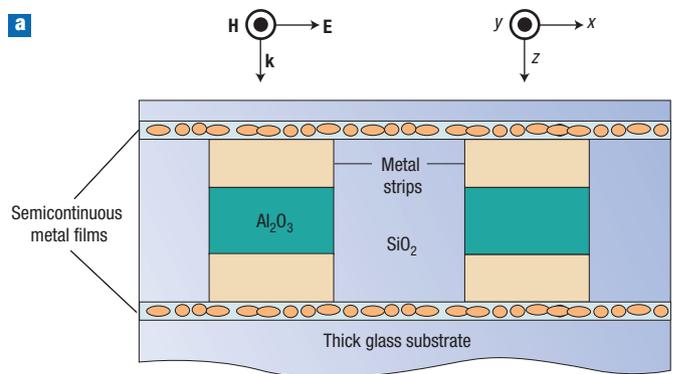
Figure 3 New designs for NIMs. **a**, Schematic representation of an array of nanostrip pairs with (semicontinuous) metal films. The structure is invariant along the y direction. Reprinted with permission from ref. 49. Copyright (2006) OSA. **b**, Schematic representation for the geometry based on pairs of cut wires (rods) and continuous wire pairs. Reprinted with permission from ref. 48. Copyright (2006) APS.

used — for the SMF with a physical thickness of 20 nm and a silver filling fraction of 65%, the calculated refractive index has a value of $n = -1.85 + 0.93i$ at $\lambda \approx 1.5$ μm[49].

Further development of optical NIMs will probably require 'smart' designs, similar to those outlined above that combine a resonant magnetic structure with a non-resonant electric structure, with the latter providing a negative permittivity in a broad spectral range including the magnetic-resonance wavelength. Another challenge to address for the development of NIM-based devices in the optical range is scaling the double-layer structures considered so far into three-dimensional (3D) objects. For this, a recent theoretical report on a greater F in 3D fishnet structures is indeed very encouraging[50].

OPTICAL NIMS WITH TUNABLITY AND GAIN

TUNABLE NIMS

To provide full operational functionality for optical NIM devices, they can be complemented by integrated tunable elements. At low terahertz frequencies, tunability has already been demonstrated through the photo-excitation of free carriers in a GaAs substrate[51]. The tunability in the optical range can be accomplished by incorporating electro-optically active materials such as liquid crystals into NIM structures. Tuning or switching and other modulation processes can be performed electro–optically or (nonlinear) all-optically by exploiting, for example, the record-high electro–optic and nonlinear optical responses in these materials[52,53]. The unique properties of liquid crystals such as compatibility with almost all materials for NIMs, very broadband transparency over a range of wavelengths from 0.4 µm to 20 µm, large optical birefringence (Δn as large as 0.6, $\Delta\varepsilon_{op} = n_o^2 - n_e^2 > 2$, where the subscripts o and e denote ordinary and extraordinary, respectively) and ultrahigh nonlinearities (refractive-index nonlinear coefficient $n_2 \approx 1\ \mathrm{cm^2\ W^{-1}}$) make them excellent candidate materials for developing both passive and active reconfigurable NIM optical elements throughout the entire optical spectrum.

NIMS WITH GAIN

Eliminating losses in optical NIMs is critical for enabling their numerous potential applications, including their applications in superlenses. We note that loss is an extremely severe detrimental factor in NIM designs. For example, to realize subwavelength resolution in a superlens, losses should decrease exponentially to obtain a linear improvement in the spatial resolution[54]. Using active media could be one way of developing low-loss NIMs and their applications.

It has been shown that energy can be transferred from gain material to propagating surface-plasmon polaritons[55–60] and to localized surface plasmons in metal nanostructures[61–63] using stimulated emission. Specifically, thin films of metals were used to confine lasing modes in quantum-cascade lasers to the gain region and also to guide the lasing modes by surface-plasmon modes[55–56]. Ramakrishna and Pendry, and independently Shamonina suggested placing gain material between the metal layers of stacked near-field superlenses[64,65] in order to remove absorption and improve the resolution of the superlens. Instead of alternating the layers of negative- and positive-index materials, the negative-index structures (such as pairs of metal rods or strips) can be 'submerged' in the gain media. For example, this could be achieved by spin coating a solution of laser dye molecules or π-conjugated polymers on top of the negative-index structures. Applying semiconductor nanocrystals as a gain material could be an alternative approach. Finally, using the strong Raman amplification in submicrometre silicon waveguides could be yet another promising approach to obtaining gain in NIMs[66].

One might question whether the metal nanostructures nullify any attempt to use gain materials close to metals, as gold nanoparticles are well known to quench fluorescence in an extremely efficient manner[67,68]. In contrast, however, working solid-state and organic semiconductor lasers show that sufficient gain can be provided so that the losses can be compensated in devices containing metal layers or nanoparticles. For instance, it has been shown that an optically pumped organic laser comprising a metal-nanoparticle distributed feedback (DFB) grating needs only a marginally increased pumping threshold (compared with organic lasers with metal-free DFB gratings) to be operative[69]. Also, the strong compensation of losses in surface plasmons of silver colloidal particles, with gain provided by dye molecules, has recently been demonstrated by the Norfolk State University and Purdue University team[63]. We therefore conclude that it should be feasible to use gain materials to compensate for the losses introduced by plasmonic nanostructures in NIMs.

In addition to absorptive losses, NIMs using plasmonic elements also have the problem of high reflection; both absorption and reflection reduce the overall transmission through the metamaterial. Whereas losses can be compensated with gain inclusions, the reflection can be suppressed by an optimized design with a matched impedance, Z. An example of an optimized NIM where the conditions $Z \to 1 + 0i$, $n' < -1$, and $|n''| << 1$ both hold for a visible wavelength has been shown in the numerical simulations of ref. 70.

Although feasible, it is still a challenge to fabricate NIMs with a sufficient level of gain. However, by further optimizing the design it should be possible to reduce the gain required. There is also the problem of amplified spontaneous emission (noise) that is expected to limit performance of NIM-based devices. However, it is known that lasers, where gain fully compensates losses, have unique, unparalleled characteristics despite the fact that amplified spontaneous emission does take place. Thus, by optimizing the structure and the gain inclusions, researchers hope to minimize losses and thus enable a family of new NIM-based devices to be developed, including the superlens, where the spatial resolution could be brought close to the ultimate limit stemming from the finite electron velocity — possibly as small as just a few nanometres[71].

NONLINEAR OPTICS IN NIMS

Here we briefly outline several nonlinear optical phenomena that can occur in NIMs because of the change in the sign of n in both the spatial and frequency domains. In the frequency domain, the optical spectra of short pulses are assumed to be so broad that the frequency region where n changes sign can be within the spectral width of the signal. The spectral components from these different domains are coupled owing to material nonlinearity, providing a new mechanism for nonlinear optics in NIMs and resulting, for example, in a new class of solitons that cannot exist in positive-index materials (PIMs)[72].

In the space domain, new nonlinear phenomena can also result from the change of refraction at the PIM–NIM interface. It has been shown that the opposite directions of the wavevector and the Poynting vector in NIMs result in extraordinary optical properties, including 'backward' phase matching and a new type of Manley–Rowe relations, which control the energy balance during propagation in nonlinear media[73]. Second harmonic generation (SHG), including nonlinear 100% mirrors based on SHG propagating against the fundamental wave, has been proposed[19,73–75], and the first experimental studies of SHG in magnetic split-ring resonator metamaterials have been reported[76].

The unusual properties of nonlinear transmission in a layered structure consisting of a slab of a PIM with Kerr-type nonlinearity and a thin (subwavelength) layer of linear NIM sandwiched between semi-infinite linear dielectrics were predicted in ref. 77. It was found that the thin layer of NIM leads to a strong increase in the hysteresis width and unidirectional, diode-like transmission of light with an enhanced operational range. These results may be useful for NIM characterization and for designing NIM-based devices, such as optical memory and optical diodes.

It has been predicted[78] that optical parametric amplification controlled by the auxiliary electromagnetic field can enable transparency, amplification and oscillation with no cavity in strongly absorbing NIMs. This opens a new means for compensating losses in NIMs. It was also shown that the opposite directions of the wavevector and the Poynting vector in such materials result in the generation of entangled pairs of left- and right-handed counter-propagating photons — a phenomenon that could find applications in quantum information.

Bringing NIMs up to the optical range and thus enabling meta-atoms to be probed with both 'hands' of light — the electric- and magnetic-field components — makes a host of new physical phenomena and applications possible, many of which were unthinkable in the past. These include, for example, a superlens allowing nanoscale imaging and nanophotolithography[79–86]. Another exciting application is related to the cloaking of objects from electromagnetic fields[86–94]. Finally, optical metamaterials can efficiently, and 'both-handedly', couple light to the nanoscale yielding a family of NIM-based devices for nanophotonics, such as nanoscale antennae, resonators, lasers, switchers, waveguides and other components that can allow the development of unparalleled methods for manipulating and controlling light at the nanoscale.

References

1. Schuster, A. *An Introduction to the Theory of Optics* (Arnold, London, 1904).
2. Lamb, H. On group-velocity. *Proc. Lond. Math. Soc.* **1,** 473–479 (1904).
3. Mandel'shtam, L. I. Group velocity in a crystal lattice. *Zh. Eksp. Teor. Fiz.* **15,** 475–478 (1945).
4. Sivukhin, D. V. The energy of electromagnetic waves in dispersive media. *Opt. Spektrosk* **3,** 308–312 (1957).
5. Veselago, V. G. The electrodynamics of substances with simultaneously negative values of ε and μ. *Sov. Phys. Uspekhi* **10,** 509–514 (1968).
6. Pendry, J. B. Negative refraction makes a perfect lens. *Phys. Rev. Lett.* **85,** 3966–3969 (2000).
7. Kosaka, H. *et al.* Superprism phenomena in photonic crystals. *Phys. Rev. B* **58,** 10096–10099 (1998).
8. Notomi, M. Theory of light propagation in strongly modulated photonic crystals: Refraction like behavior in the vicinity of the photonic band gap. *Phys. Rev. B* **62,** R10696–R10705 (2000).
9. Gralak, B., Enoch, S & Tayeb, G. Anomalous refractive properties of photonic crystals. *J. Opt. Soc. Am. A* **17,** 1012–1020 (2000).
10. Luo, C. *et al.* All-angle negative refraction without negative effective index. *Phys. Rev. B* **65,** 201104 (2002).
11. Berrier, A. *et al.* Negative refraction at infrared wavelengths in a two-dimensional photonic crystal. *Phys. Rev. Lett.* **93,** 073902 (2004).
12. Smith, D. R. *et al.* Limitations on sub-diffraction imaging with a negative refractive index slab. *Appl. Phys. Lett.* **82,** 1506–1508 (2003).
13. Luo, C. *et al.* Sub-wavelength imaging in photonic crystals. *Phys. Rev. B* **68,** 045115 (2003).
14. Lu, Z. *et al.* Three-dimensional sub-wavelength imaging by a photonic-crystal flat lens using negative refraction at microwave frequencies. *Phys. Rev. Lett.* **95,** 153901 (2005).
15. Eleftheriades, G. V., Iyer, A. K. & Kremer, P. C. Planar negative refractive index media using periodically L–C loaded transmission lines. *IEEE Trans. Microwave Theory Tech.* **50,** 2702–2712 (2002).
16. Alù, A. & Engheta, N. Optical nanotransmission lines: Synthesis of planar left-handed metamaterials in the infrared and visible regimes. *J. Opt. Soc. Am. B* **23,** 571–583 (2006).
17. Depine, R. A. & Lakhtakia, A. A new condition to identify isotropic dielectric-magnetic materials displaying negative phase velocity. *Microwave Opt. Technol. Lett.* **41,** 315–316 (2004).
18. McCall, M. W., Lakhtakia, A. & Weiglhofer, W. S. The negative index of refraction demystified. *Eur. J. Phys.* **23,** 353–359 (2002).
19. Agranovich, V. M. *et al.* Linear and nonlinear wave propagation in negative refraction metamaterials. *Phys. Rev. B* **69,** 165112 (2004).
20. Podolskiy, V. A. & Narimanov, E. E. Strongly anisotropic waveguide as a nonmagnetic left-handed system. *Phys. Rev. B* **71,** 201101 (2005).
21. Shin, H. & Fan, S. All-angle negative refraction for surface plasmon waves using a metal-dielectric-metal structure. *Phys. Rev. Lett.* **96,** 073907 (2006).
22. Pendry, J. B. *et al.* Magnetism from conductors and enhanced nonlinear phenomena. *IEEE Trans. Microwave Theory Tech.* **47,** 2075–2084 (1999).
23. Smith, D. R. *et al.* Composite medium with simultaneously negative permeability and permittivity. *Phys. Rev. Lett.* **84,** 4184–4187 (2000).
24. Shelby, R. A., Smith, D. R. & Schultz, S. Experimental verification of a negative index of refraction. *Science* **292,** 77–79 (2001).
25. Yen, T. J. *et al.* Terahertz magnetic response from artificial materials. *Science* **303,** 1494–1496 (2004).
26. Zhang, S. *et al.* Midinfrared resonant magnetic nanostructures exhibiting a negative permeability. *Phys. Rev. Lett.* **94,** 037402 (2005).
27. Linden, S. *et al.* Magnetic response of metamaterials at 100 terahertz. *Science* **306,** 1351–1353 (2004).
28. Enkrich, C. *et al.* Magnetic metamaterials at telecommunication and visible frequencies. *Phys. Rev. Lett.* **95,** 203901 (2005).
29. Kildishev, A. V. *et al.* Negative refractive index in optics of metal–dielectric composites. *J. Opt. Soc. Am. B* **23,** 423–433 (2006).
30. Shvets, G. Urzhumov, Y. A. Negative index meta-materials based on two-dimensional metallic structures. *J. Opt. A* **8,** S122–S130 (2006).
31. Yuan, H.-K. *et al.* A negative permeability material at red light. Preprint at <http://arxiv.org/abs/physics/0610118> (2006).
32. *International Commission on Illumination (1987): International Lighting Vocabulary* 4th edn (CIE, Vienna, 1987).
33. Podolskiy, V. A., Sarychev, A. K. & Shalaev, V. M. Plasmon modes in metal nanowires and left-handed materials. *J. Nonlin. Opt. Phys. Mater.* **11,** 65–74 (2002).
34. Grigorenko, A. N. *et al.* Nanofabricated media with negative permeability at visible frequencies. *Nature* **438,** 335–338 (2005).
35. Grigorenko, A. Negative refractive index in artificial metamaterials. *Opt. Lett.* **31,** 2483–2485 (2006).
36. Kildishev, A. V. *et al.* Comment on 'Negative refractive index in artificial metamaterials'. Preprint at <http://arxiv.org/abs/physics/0609234> (2006).
37. Shalaev, V. M. *et al.* Negative index of refraction in optical metamaterials. *Opt. Lett.* **30,** 3356–3358 (2005).
38. Zhang, S. *et al.* Experimental demonstration of near-infrared negative-index metamaterials. *Phys. Rev. Lett.* **95,** 137404 (2005).
39. Lagarkov, A. N. & Sarychev, A. K. Electromagnetic properties of composites containing elongated conducting inclusions. *Phys. Rev. B* **53,** 6318–6336 (1996).
40. Panina, L. V., Grigorenko, A. N. & Makhnovskiy, D. P. Optomagnetic composite medium with conducting nanoelements. *Phys. Rev. B* **66,** 155411 (2002).
41. Podolskiy, V. A., Sarychev, A. K. & Shalaev, V. M. Plasmon modes and negative refraction in metal nanowire composites. *Opt. Express* **11,** 735–745 (2003).
42. Engheta, N., Salandrino, A. & Alu, A. Circuit elements at optical frequencies: Nanoinductors, nanocapacitors, and nanoresistors. *Phys. Rev. Lett.* **95,** 095504 (2005).
43. Zhang, S. *et al.* Demonstration of metal-dielectric negative-index metamaterials with improved performance at optical frequencies. *J. Opt. Soc. Am. B* **23,** 434–438 (2006).
44. Dolling, G. *et al.* Low-loss negative-index metamaterial at telecommunication wavelengths. *Opt. Lett.* **31,** 1800–1802 (2006).
45. Zhang, S. *et al.* Near-infrared double negative metamaterials. *Opt. Express* **13,** 4922–4930 (2005).
46. Dolling, G. *et al.* Simultaneous negative phase and group velocity of light in a metamaterial. *Science* **312,** 892–894 (2006).
47. Dolling G., Wegener, M., Soukoulis, C. M. & Linden, S. Negative-index material at 780 nm wavelength. Preprint at <http://arxiv.org/abs/physics/0607135> (2006).
48. Zhou, J. *et al.* Negative index materials using simple short wire pairs. *Phys. Rev. B* **73,** 041101(R) (2006).
49. Chettiar, U. K. *et al.* Negative index metamaterial combining magnetic resonators with metal films. *Opt. Express* **14,** 7872–7877 (2006).
50. Zhang, S. *et al.* Optical negative-index bulk metamaterials consisting of 2D perforated metal-dielectric stacks. *Opt. Express* **14,** 6778–6787 (2006).
51. Padilla, W. J. *et al.* Dynamical electric and magnetic metamaterial response at THz frequencies, *Phys. Rev. Lett.* **96,** 107401 (2006).
52. Khoo, I. C. *Liquid Crystals: Physical Properties and Nonlinear Optical Phenomena* (Wiley, New York, 1995).
53. Khoo, I. C. *et al.* Supra-nonlinear photorefractive response of single-wall carbon nanotube- and C60-doped nematic liquid crystal. *Appl. Phys. Lett.* **82,** 3587–3589 (2003).
54. Podolskiy, V. A. & Narimanov, E. E. Near-sighted superlens, *Opt. Lett.* **30,** 75–77 (2005).
55. Sirtori, C. *et al.* Long-wavelength (λ = 8–11.5 μm) semiconductor lasers with waveguides based on surface plasmons. *Opt. Lett.* **23,** 1366–1368 (1998).
56. Tredicucci, A. *et al.* Single-mode surface-plasmon laser. *Appl. Phys. Lett.* **76,** 2164–2166 (2000).
57. Sudarkin, A. N. & Demkovich, P. A. Excitation of surface electromagnetic waves on the boundary of a metal with an amplifying medium. *Sov. Phys. Tech. Phys.* **34,** 764–766 (1989).
58. Nezhad, M. P., Tetz, K. & Fainman, Y. Gain assisted propagation of surface plasmon polaritons on planar metallic waveguides. *Opt. Express* **12,** 4072–4079 (2004).
59. Avrutsky, I. Surface plasmons at nanoscale relief gratings between a metal and a dielectric medium with optical gain. *Phys. Rev. B* **70,** 155416 (2004).
60. Seidel, J., Grafström, S. & Eng, L. Stimulated emission of surface plasmons at the interface between a silver film and an optically pumped dye solution. *Phys. Rev. Lett.* **94,** 177401 (2005).
61. Bergman, D. J. & Stockman, M. I. Surface plasmon amplification by stimulated emission of radiation: Quantum generation of coherent surface plasmons in nanosystems. *Phys. Rev. Lett.* **90,** 027402 (2003).
62. Lawandy, N. M. Localized surface plasmon singularities in amplifying media. *Appl. Phys. Lett.* **85,** 5040–5042 (2004).
63. Noginov, M. A. *et al.* Enhancement of surface plasmons in an Ag aggregate by optical gain in a dielectric medium. *Opt. Lett.* **31,** 3022–3024 (2006).
64. Ramakrishna, S. A. & Pendry, J. B. Removal of absorption and increase in resolution in a near-field lens via optical gain. *Phys. Rev. B* **67,** 201101 (2003).
65. Shamonina E. *et al.* Imaging, compression and Poynting vector streamlines for negative permittivity materials. *Elec. Lett.* **37,** 1243–1244 (2001).
66. Espinola, R. L. *et al.* Raman amplification in ultrasmall silicon-on-insulator wire waveguides. *Opt. Express* **12,** 3713–3718 (2004).
67. Dulkeith, E. *et al.* Fluorescence quenching of dye molecules near gold nanoparticles: Radiative and nonradiative effects. *Phys. Rev. Lett.* **89,** 203002 (2002).
68. Imahori, H. *et al.* Structure and photophysical properties of porphyrin-modified metal nanoclusters with different chain lengths. *Langmuir* **20,** 73–81 (2004).
69. Stehr, J. *et al.* A low threshold polymer laser based on metallic nanoparticle gratings. *Adv. Mater.* **15,** 1726 (2003).
70. Klar, T. A. *et al.* Negative-index metamaterials: Going optical. *IEEE J. Selec. Top. Quant. Electron.* **12,** (2006).
71. Larkin, I. A. & Stockman, M. I. Imperfect perfect lens. *Nano Lett.* **5,** 339–343 (2005).
72. Gabitov, I. R. *et al.* Double-resonant optical materials with embedded metal nanostructures. *J. Opt. Soc. Am. B* **23,** 535–542 (2006).

73. Popov, A. K. & Shalaev, V. M. Negative-index metamaterials: Second-harmonic generation, Manley-Rowe relations and parametric amplification. *Appl. Phys. B* **84,** 131–137 (2006).

74. Shadrivov, I. V., Zharov, A. A. & Kivshar, Y. S. Second-harmonic generation in nonlinear left-handed metamaterials. *J. Opt. Soc. Am. B* **23,** 529–534 (2006).

75. Zharov, A. A. *et al.* Subwavelength imaging with opaque nonlinear left-handed lenses. *Appl. Phys. Lett.* **87,** 091104 (2005).

76. Klein, M. W. *et al.* Second-harmonic generation from magnetic metamaterials. *Science* **313,** 502–504 (2006).

77. Litchinitser, N. M. *et al.* Effect of negative-index thin film on optical bistability. *Opt. Lett.* (in the press); preprint at <http://arxiv.org/abs/physics/0607177>.

78. Popov, A. K. & Shalaev V. M. Compensating losses in negative-index metamaterials with optical parametric amplification. *Opt. Lett.* **31,** 2169–2171 (2006).

79. Fang, N., Lee, H. & Zhang, X. Sub-diffraction-limited optical imaging with a silver superlens. *Science* **308,** 534–537 (2005).

80. Melville, D. O. S. & Blaikie, R. J. & Wolf, C. R. Submicron imaging with a planar silver lens. *Appl. Phys. Lett.* **84,** 4403–4405 (2004).

81. Melville, D. O. S., Blaikie, R. J. Super-resolution imaging through a planar silver layer. *Opt. Express* **13,** 2127–2134 (2005).

82. Taubner T. *et al.* Near-field microscopy through a SiC superlens. *Science* **313,** 1595 (2006).

83. Cai, W., Genov, D. A. & Shalaev, V. M. Superlens based on metal-dielectric composites. *Phys. Rev. B* **72,** 193101 (2005).

84. Durant, S., Liu, Z., Fang, N. & Zhang, X. Theory of optical imaging beyond the diffraction limit with a far-field superlens. *Proc. SPIE* **6323,** 63231H (2006).

85. Jacob Z., Alekseyev, L. V. & Narimanov, E. Optical hyperlens: Far-field imaging beyond the diffraction limit. *Opt. Express* **14,** 8247–8256 (2006).

86. Salandrino, A. & Engheta, N. Far-field subdiffraction optical microscopy using metamaterial crystals: Theory and simulations. *Phys. Rev. B* **74,** 075103 (2006).

87. Nicorovici, N. A., McPhedran, R. C. & Milton, G. W. Optical and dielectric properties of partially resonant composites. *Phys. Rev. B* **49,** 8479–8482 (1994).

88. Milton, G. W. *et al.* A proof of superlensing in the quasistatic regime, and limitations of superlenses in this regime due to anomalous localized resonance. *Proc. Roy. Soc. A* **461,** 3999–4034 (2005).

89. Alù, A. & Engheta, N. Achieving transparency with plasmonic and metamaterial coatings. *Phys. Rev. E* **95,** 016623 (2005).

90. Garcia de Abajo, F. J. *et al.* Tunneling mechanism of light transmission through metal films. *Phys. Rev. Lett.* **95,** 067403 (2005).

91. Pendry, J. B., Shurig, D. & Smith D. R. Controlling electromagnetic fields. *Science* **312,** 1780–1782 (2006).

92. Leonhardt, U. Optical conforming mapping. *Science* **312,** 1777–1780 (2006).

93. Schurig, D. *et al.* Metamaterial electromagnetic cloak at microwave frequencies. *Science* **314,** 977–980 (2006).

94. Cai, W., Chettiar, U. K., Kildishev, A. V. & Shalaev, V. M. Optical cloaking with non-magnetic metamaterials. Preprint at <http://arxiv.org/abs/physics/0611242> (2006).

95. Liu, Z. *et al.* Rapid growth of evanescent wave with a silver superlens. *Appl. Phys. Lett.* **83,** 5184–5186 (2003).